

# Deriving room temperature excitation spectra for photosystem I and photosystem II fluorescence in intact leaves from the dependence of $F_V/F_M$ on excitation wavelength

Erhard E. Pfündel

Received: 24 March 2009 / Accepted: 1 June 2009 / Published online: 20 June 2009  
© Springer Science+Business Media B.V. 2009

**Abstract** The  $F_0$  and  $F_M$  level fluorescence from a wild-type barley, a Chl *b*-less mutant barley, and a maize leaf was determined from 430 to 685 nm at 10 nm intervals using pulse amplitude-modulated (PAM) fluorimetry. Variable wavelengths of the pulsed excitation light were achieved by passing the broadband emission of a Xe flash lamp through a birefringent tunable optical filter. For the three leaf types, spectra of  $F_V/F_M (= (F_M - F_0)/F_M)$  have been derived: within each of the three spectra of  $F_V/F_M$ , statistically meaningful variations were detected. Also, at distinct wavelength regions, the  $F_V/F_M$  differed significantly between leaf types. From spectra of  $F_V/F_M$ , excitation spectra of PS I and PS II fluorescence were calculated using a model that considers PS I fluorescence to be constant but variable PS II fluorescence. The photosystem spectra suggest that LHC II absorption results in high values of  $F_V/F_M$  between 470 and 490 nm in the two wild-type leaves but the absence of LHC II in the Chl *b*-less mutant barley leaf decreases the  $F_V/F_M$  at these wavelengths. All three leaves exhibited low values of  $F_V/F_M$  around 520 nm which was tentatively ascribed to light absorption by PS I-associated carotenoids. In the 550–650 nm region, the  $F_V/F_M$  in the maize leaf was lower than in the barley wild-type leaf which is explained with higher light absorption by PS I in maize, which is a NADP-ME  $C_4$  species, than in barley, a  $C_3$  species. Finally, low values of  $F_V/F_M$  at 685 nm in maize leaf and in the Chl *b*-less mutant barley leaf are in agreement with preferential PS I absorption at this wavelength. The potential use of spectra of the  $F_V/F_M$  ratio to derive information on spectral absorption properties of PS I and PS II is discussed.

**Keywords** Chlorina mutant · *Hordeum vulgare* · In vivo · Photosystem I · Photosystem II · Spectroscopy · *Zea mays*

## Abbreviations

Chl <i>a</i> and <i>b</i>	Chlorophyll <i>a</i> and <i>b</i>
LHC I and LHC II	Light-harvesting complex I and II
PAM	Pulse amplitude modulated
PS I and PS II	Photosystem I and II

## Introduction

Light energy absorbed by photosynthetic pigments is partially re-emitted by PS II as Chl *a* fluorescence. In dark-acclimated leaves, the intensity of Chl *a* fluorescence depends mainly on the state of PS II reaction centers: when PS II reaction centers are “open,” that is when they can efficiently use excitation energy for charge separation,  $F_0$  level fluorescence is observed. The  $F_M$  level of fluorescence can only be measured when all PS II reaction centers are “closed,” that is when they are not capable of stable charge separation (Govindjee 2004). At the same excitation light flux,  $F_M$  level fluorescence is about fivefold higher than  $F_0$  fluorescence because the closed reaction centers cannot trap excitation energy but the open ones compete effectively with fluorescence emission for excitation energy (Butler 1978; Schreiber 2004).

The Chl *a* fluorescence intensities depend on the PS II reaction center state has been exploited by Kitajima and Butler (1975a) who introduced the fluorescence ratio of  $F_V/F_M$ , where  $F_V = F_M - F_0$ , as a measure for the photochemical quantum yield of PS II in dark-acclimated material. Later, additional fluorescence ratio parameters have been introduced to assess the utilization of absorbed

E. E. Pfündel (✉)  
Heinz Walz GmbH, Eichenring 6, 91090 Effeltrich, Germany  
e-mail: epfuendel@walz.com

photons by the photosynthetic apparatus in the light-acclimated state [see, Baker (2008), for a recent review].

In contrast to PS II fluorescence, PS I fluorescence is considered to be rather constant because the flow of absorbed light energy into the open PS I reaction center is similar than the flow into the closed PS I reaction center (Dau 1994; Trissl 1997). Therefore, the contribution of PS I to total fluorescence (PS I plus PS II) under  $F_0$  conditions should be higher than the contribution to total fluorescence at  $F_M$  conditions. Indeed, at wavelengths longer than 700 nm, PS I fluorescence is approximately 30–50% of total  $F_0$  fluorescence, with high PS I fluorescence percentages in leaves with high PS I/PS II concentration ratios, but the PS I contribution to the  $F_M$  level is only around 10% (Agati et al. 2000; Franck et al. 2002; Genty et al. 1990; Peterson et al. 2001; Pfündel 1998; Rappaport et al. 2007).

Both the PS I and PS II fluorescence intensities are a function of the absorption efficiency of their light-harvesting antennae. Action spectra indicate that the absorption spectra of PS I and PS II differ (Boichenko 1998; Ried 1971; Schreiber and Vidaver 1974). Therefore, the relative contributions of PS I and PS II to the total fluorescence are expected to vary with excitation wavelength. Since PS I fluorescence variations would affect predominantly the  $F_0$  fluorescence and to a much lesser degree the  $F_M$  fluorescence (see above), a simple way to investigate the wavelength-dependent relationship between PS I and PS II absorption is to record spectra of fluorescence quotients of  $F_0$  and  $F_M$ .

Indeed, to test for the presence of PS I fluorescence at room temperature, Zucchelli et al. (1988) have measured  $F_0/F_M$  spectra between 400 and 520 nm with 682 nm as the detection wavelength using a conventional fluorometer. The authors reported a rather featureless spectrum from which they have derived that PS I fluorescence can be neglected. The present study newly investigates the issue of wavelength-dependent PS I/PS II fluorescence ratios by recording spectra of  $F_v/F_M$  derived from pulse amplitude-modulated (PAM) fluorescence measurements at wavelengths >700 nm. The study employs a Xe flash lamp in combination with tunable birefringent filter as the excitation light. The results show that the  $F_v/F_M$  is dependent on excitation wavelength and that this dependency most likely originates from the different spectral absorption properties of PS I and PS II.

## Materials and methods

### Plants

Seeds of wild-type barley, *Hordeum vulgare* L. cv. Donaria, and the Chl *b*-less mutant chlorina-f2 2800, which is rooted

in the Donaria variety (Simpson et al. 1985), were obtained from the Institut für Pflanzengenetik und Kulturpflanzenforschung, Gatersleben, Germany. Maize seeds (*Zea mays* L., hybrid corn cv. “Oural FA0230”) were purchased from Deutsche Saatveredelung, Lippstadt, Germany. Seeds were grown in the laboratory in pots of 12 cm diameter containing commercially available soil (Kultursubstrat Typ KS II, Terrasan, Rain am Lech, Germany). Plants were watered daily. Maximum day light intensities were  $50 \mu\text{mol m}^{-2} \text{s}^{-1}$  around noon but temporarily reached  $500 \mu\text{mol m}^{-2} \text{s}^{-1}$  when plants were directly exposed to the sun during late afternoon hours. The top quarter of 12-day-old leaves was investigated. On the day of experiments, exposure of plants to direct sunlight was prevented. Immediately before starting experiments, plants were kept under low light conditions ( $3 \mu\text{mol m}^{-2} \text{s}^{-1}$ ) for at least 1.5 h.

### Experimental design for fluorescence measurements

Fluorescence was measured using an XE-PAM fluorimeter (Walz, Effeltrich, Germany; see Schreiber et al. (1993) for an instrument description). The fluorimeter was operated by the WinControl V2.08 software via a PAM data-acquisition system PDA-100 (both Walz).  $F_0$  and  $F_M$  level fluorescence was recorded using 2 and 64 Hz excitation flash frequency, respectively. The pulsed excitation beam was passed through two Calflex X filters (Balzers, Liechtenstein), an SP695 and a GG19 filter (both Schott, Mainz, Germany), a UV-blocking filter (Balzers, Liechtenstein), and a VariSpec VIS-10 tunable filter (LOT-Oriel, Darmstadt, Germany). The VariSpec filter was controlled by the VsGui Program via a VariSpec Electronics Controller (both LOT-Oriel). Excitation light was guided by a Perspex rod into the sample compartment of an ED-101US/M Optical Unit (Walz).

Fluorescence emission light was collected, at right-angles to the path of excitation light, by another Perspex rod and guided to the XE-PAM photodetector which was attached to the ED-101US/M Optical Unit. The following filters were mounted in front of the photodetector: R65 (thickness 1 mm, Balzers), RG645 (thickness 3 mm, Schott), and RG9 (thickness 1 mm, Schott). The latter filter limits fluorescence detection to wavelengths longer than 700 nm. Saturation pulses of white light (wavelengths < 695 nm) were delivered by the halogen lamp of an XE-AL unit (Walz) which was connected by fiber optics to the light port opposite to the port for the measuring light.

### Characterization of excitation light

The VariSpec VIS-10 tunable filter was varied between 400 and 720 nm at 10 nm intervals which corresponds to 33

different settings per scan. For all 33 settings, the spectra of the excitation light were recorded by a diode array-type spectrometer with 2.4 nm spectral resolution (Multi-Channel-Spektrometer MCS 55/m, Carl Zeiss, Jena, Germany), which was operated by special software (MMS Betriebselektronik demonstration program V5.1, Tec5 Sensorik und Systemtechnik, Oberursel, Germany). Wavelength accuracy of the spectrometer was confirmed by recording the 633 nm emission line of a 5 mW He–Ne laser (provided by LOT Oriol).

In order to record excitation light spectra, the flash lamp of the XE-PAM with all excitation filters in place was attached to the fiber optics of the Multi-Channel-Spektrometer. Also, the emission spectrum from a standard lamp was recorded (Li-Cor Spectral Irradiance Lamp 1800-02L, Li-Cor, Lincoln, Nebraska, USA). Then, the response curve of the spectrometer was established by dividing the experimental lamp spectrum by the lamp's known standard emission spectrum converted in  $\mu\text{mol} (\text{m}^2 \text{s})^{-2}$ . Finally, the effects of the spectrometer's spectral response on light spectra were corrected by dividing the light spectra by the spectrometer's response curve. The corrected light spectra were integrated to obtain for each filter setting the relative intensities of excitation light (relative photon flux:  $I_{\text{REL}}(\lambda_{\text{EX}})$ ; see Fig. 1). The effective wavelength ( $\lambda_{\text{EX}}$ ) for each filter setting was calculated according to

$$\lambda_{\text{EX}} = \frac{\sum I(\lambda) \cdot \lambda}{\sum I(\lambda)},$$

where  $I(\lambda)$  and  $\lambda$  represent the relative intensity and wavelength, respectively, of the excitation light spectrum.

### Fluorescence measurements

One leaf per plant type was investigated. For measurements, a plant pot was placed beneath the ED-101US/M Optical Unit. The top part of one attached leaf was inserted through the bottom part of the ED-101US/M Optical Unit into the sample compartment. In the sample compartment, excitation light was introduced at an angle of  $45^\circ$  to the upper leaf surface. Fluorescence from the upper leaf side was detected at right-angles to the excitation light. In order to elicit  $F_M$  fluorescence, strong white light pulses of 0.6 s duration were applied at an angle of  $45^\circ$  to the lower leaf surface. During the pulse, the photon flux densities, as measured by a US-SQS/WB Spherical Micro Quantum Sensor (Walz), were 9500 and 1000  $\mu\text{mol} (\text{m}^2 \text{s})^{-2}$  at the lower and upper leaf surfaces, respectively. In comparison, it has been reported that a photon flux density of 1000  $\mu\text{mol} (\text{m}^2 \text{s})^{-2}$  is sufficient to evoke maximum  $F_V/F_M$  values in fully dark-acclimated leaves (Karageorgou et al. 2007).

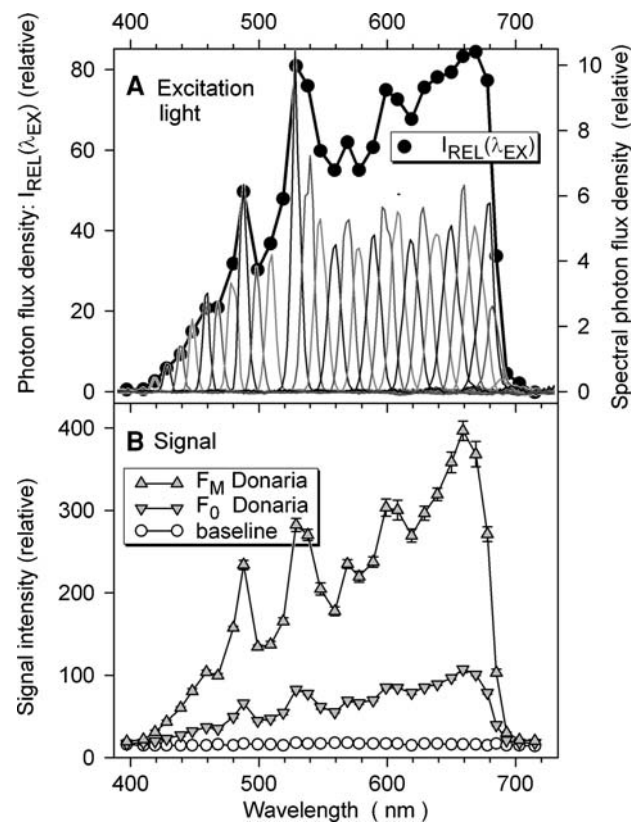


**Fig. 1** Spectra of excitation light (a) and unprocessed measuring signals (b). Panel A shows the spectra of relative photon flux densities of measuring light corresponding to the 33 filter settings used. The relative photon flux densities, calculated by integration of photon flux spectra, are drawn as dots in A. Wavelength position of photon flux densities were computed as described in [Material and methods](#). Panel B shows the mean  $F_M$  and  $F_0$  fluorescence (upward and downward triangles, respectively) of a wild-type barley leaf (“Donaria”) plotted against the wavelength of excitation light. The data of  $F_M$  and  $F_0$  are means of four scans of the same leaf spot. Error bars represent 95% confidence intervals: at low signal intensities ( $<150$ ), error bars are hidden by symbols. In B, also a single scan of the signal obtained with the blank sample holder is shown (open round symbols, “baseline”)

Measurements of  $F_0$  and  $F_M$  were started at the shortest wavelength setting of the tunable filter (400 nm). The wavelength of excitation light was increased to the highest setting (720 nm) using 10 nm increments. The dark interval between two  $F_0$  and  $F_M$  determinations was 60 s. The first wavelength scan was followed by a reverse scan from long to short wavelengths. In the same manner, two more spectra were recorded resulting in a total of 4 spectra per leaf. Also, one wavelength scan with a blank XE-SH-UV sample holder (Walz) was recorded.

### Statistics

Differences between samples of data were statistically evaluated using two-sided Student's *t*-test for samples of

equal variance. Error bars in all graphs correspond to 95% confidence intervals calculated according to

$$95\%CI = \frac{t(0.05, 2, n - 1) \cdot \sigma}{\sqrt{n - 1}},$$

where the “ $t(0.05, 2, n - 1)$ ” is the value of the t distribution at a significant level of 0.05, double-sided testing and the degree of freedom of  $(n - 1)$ . Standard deviation is represented by  $\sigma$  and  $n$  is the number of observations.

### Theoretical considerations

In this section, expressions for the dependence on excitation wavelength of PS I and PS II Chl *a* fluorescence are derived. These equations will then be used to describe the dependence on excitation wavelength of total leaf fluorescence and of the ratio of  $F_V/F_M$ . Eventually, formula for the apparent excitation spectra of PS I and PS II is developed.

#### PS II fluorescence

In dark-acclimated leaves, the level of PS II fluorescence essentially depends on the state of PS II reaction centers (photochemical fluorescence quenching) but, generally, variation in PS II fluorescence intensity can also occur due to non-photochemical quenching of fluorescence (Baker 2008; Dau 1994; Krause and Jahns 2004) and changes in PS II absorption cross section due to state transitions (Allen 1992; Haldrup et al. 2001; Horton and Black 1981). The latter two mechanisms are not considered here because their activation requires minutes of continuous illumination which was not applied in the present experiments.

As PS II absorption varies with wavelength, both, the minimum and maximum levels of PS II fluorescence depend on the wavelength of excitation light,  $\lambda_{EX}$ . In order to indicate this, PS II fluorescence at  $F_0$  and  $F_M$  conditions is denoted as  $F_0^{PS2}(\lambda_{EX})$  and  $F_M^{PS2}(\lambda_{EX})$ , respectively. At constant excitation intensity,  $I(\lambda_{EX})$ , the  $F_0^{PS2}(\lambda_{EX})$  is lower than the  $F_M^{PS2}(\lambda_{EX})$  because the open reaction centers, but not the closed ones, compete effectively with fluorescence for excitation energy (Butler 1978; Schreiber 2004). In other words, excitation energy in PS II with open reaction centers is converted into fluorescence at the yield,  $\Phi_{F_0}^{PS2}$ , which is lower than the  $\Phi_{F_M}^{PS2}$ , which is the fluorescence yield of PS II with a closed reaction center.

It is important to recall that the XE-PAM instrument utilized here, like all PAM-type fluorimeters, excites fluorescence by microsecond excitation flashes of constant intensity, and it detects only the fluorescence induced by these flashes. The excitation flashes are separated by relatively large dark periods so that the excitation light alone represents a very low integrated light intensity under which

the PS II reaction centers stay open so that  $F_0^{PS2}(\lambda_{EX})$  fluorescence is measured. In order to determine  $F_M^{PS2}(\lambda_{EX})$ , PSII reaction centers are closed by a 0.6 s intense white light pulses. The fluorescence excited by the strong light pulse is not measured by the XE-PAM fluorimeter. Hence, at a given wavelength,  $\lambda_{EX}$ , the excitation intensity which is effective for the measured signal,  $I(\lambda_{EX})$ , is constant under  $F_0$  and  $F_M$  conditions. This implies that the measured fluorescence signal is proportional to the fluorescence yield; however, the  $I(\lambda_{EX})$ , varies with changing  $\lambda_{EX}$  (see Fig. 1a.) Presupposing that PS II light absorption at  $\lambda_{EX}$ ,  $A^{PS2}(\lambda_{EX})$ , is constant under  $F_0$  and  $F_M$  conditions, the two measured PS II fluorescence levels are described by Eqs. 1 and 2:

$$F_0^{PS2}(\lambda_{EX}) = I(\lambda_{EX}) \cdot A^{PS2}(\lambda_{EX}) \cdot \Phi_{F_0}^{PS2}, \quad (1)$$

$$F_M^{PS2}(\lambda_{EX}) = I(\lambda_{EX}) \cdot A^{PS2}(\lambda_{EX}) \cdot \Phi_{F_M}^{PS2}. \quad (2)$$

#### PS I fluorescence

Different from PS II, open PS I reaction centers trap excitation energy with similar efficiency as closed ones, and hence, comparable PS I fluorescence quantum yields,  $\Phi_F^{PS1}$ , exist under  $F_0$  and  $F_M$  conditions (Dau 1994; Trissl 1997). Therefore, a single equation describes PS I fluorescence,  $F^{PS1}(\lambda_{EX})$ , under  $F_0$  and  $F_M$  conditions. In an analogous manner to Eqs. 1 and 2, the  $F^{PS1}(\lambda_{EX})$  is given by Eq. 3:

$$F^{PS1}(\lambda_{EX}) = I(\lambda_{EX}) \cdot A^{PS1}(\lambda_{EX}) \cdot \Phi_F^{PS1}, \quad (3)$$

where the  $A^{PS1}(\lambda_{EX})$  is the PS I light absorption at  $\lambda_{EX}$ .

Despite of constant  $\Phi_F^{PS1}$ , PS I fluorescence may vary if a significant portion of PS II excitation energy is transferred to PS I (“spillover”; Butler 1978). In this case, closure of PS II reaction centers would increase the excitation energy flow to PS I leading to higher PS I fluorescence under  $F_M$  conditions than under  $F_0$  conditions. The latter view is supported by Butler and Kitajima (1975) who observed, at low temperature (77 K), that far-red fluorescence increased up to 40% during PS II reaction center closure. The authors have attributed this increase to PS I fluorescence because far-red emission has been considered to originate almost completely in PS I (cf. Govindjee and Yang 1966; Mukerji and Sauer 1989).

Franck et al. (2002), however, have argued that far-red fluorescence at 77 K includes a noticeable portion of highly variable PS II emission so that PS I variable fluorescence is smaller than the total variable far-red fluorescence. At room temperature, Anderson and Melis (1983), from similar kinetic studies of PS I photochemistry in both pure PS I preparations and in isolated thylakoids, have deduced that PS II-to-PS I excitation energy transfer is

small. Further, Joliet et al. (1968), from the observation of similar PS I action spectra at different closure states of PS II reactions centers, inferred the absence of significant rates of PS II-to-PS I energy transfer. Moreover, Trissl and Wilhelm (1993) have suggested that inefficient PS II-to-PS I excitation energy transfer is due to lateral segregation of PS I and PS II in higher plant chloroplasts, and that minimum losses of excitation energy to PS I is prerequisite for the high photochemical yield of PS II in these chloroplasts. Thus, these latter publications strongly suggest that variable PS I fluorescence at room temperature is too insignificant to be considered here; hence, PS I fluorescence can indeed be treated as being constant.

Leaf fluorescence

Both PS I and PS II contribute to leaf fluorescence. Therefore, leaf fluorescences at the  $F_0$  level,  $F_0(\lambda_{EX})$ , and the  $F_M$  level,  $F_M(\lambda_{EX})$ , are described by Eqs. 4 and 5, respectively.

$$F_0(\lambda_{EX}) = F_{F_0}^{PS2}(\lambda_{EX}) + F^{PS1}(\lambda_{EX}), \tag{4}$$

$$F_M(\lambda_{EX}) = F_{F_M}^{PS2}(\lambda_{EX}) + F^{PS1}(\lambda_{EX}). \tag{5}$$

Expressing the variable normalized to maximum fluorescence,  $F_V(\lambda_{EX})/F_M(\lambda_{EX})$ , using Eqs. 4 and 5 followed by replacing the terms for PS I and PS II fluorescence by Eqs. 1–3 yields

$$\frac{F_V(\lambda_{EX})}{F_M(\lambda_{EX})} = \frac{F_M(\lambda_{EX}) - F_0(\lambda_{EX})}{F_M(\lambda_{EX})} = \frac{\Phi_V^{PS2}}{1 + \frac{A^{PS1}(\lambda_{EX}) \cdot \Phi_F^{PS1}}{A^{PS2}(\lambda_{EX}) \cdot \Phi_F^{PS2}}} \tag{6}$$

In Eq. 6,  $\Phi_V^{PS2}$  is defined as  $(\Phi_{F_M}^{PS2} - \Phi_{F_0}^{PS2}) / \Phi_{F_M}^{PS2}$  and, thus, represents the normalized variable fluorescence yield of pure PS II. Note that Eq. 6 predicts that  $F_V(\lambda_{EX})/F_M(\lambda_{EX})$  depends on the excitation wavelength provided that  $\Phi_F^{PS1} > 0$  and the PS I/PS II absorption ratio varies with wavelength. Rearrangement of Eq. 6 results in an expression (Eq. 7) for the relative contribution of PS I to  $F_M$  fluorescence:

$$\frac{F^{PS1}(\lambda_{EX})}{F_M(\lambda_{EX})} = 1 - \frac{1}{\Phi_V^{PS2}} \cdot \frac{F_V(\lambda_{EX})}{F_M(\lambda_{EX})}. \tag{7}$$

Further rearrangement leads to Eq. 8 describing the portion of PS I fluorescence contributing to the  $F_0$  fluorescence:

$$\frac{F^{PS1}(\lambda_{EX})}{F_0(\lambda_{EX})} = \left(1 - \frac{1}{\Phi_V^{PS2}} \cdot \frac{F_V(\lambda_{EX})}{F_M(\lambda_{EX})}\right) / \left(1 - \frac{F_V(\lambda_{EX})}{F_M(\lambda_{EX})}\right). \tag{8}$$

Computations of relative PS I portions according to Eqs. 7 and 8 require that  $\Phi_V^{PS2}$  is known. For  $\Phi_V^{PS2}$ , a value of 0.88 was determined with fully differentiated leaves from *Flaveria* species grown in sun-exposed conditions in a

greenhouse (Pfündel 1998). Franck et al. (2002) determined for  $\Phi_V^{PS2}$  a value of 0.83 with 7-day-old barley leaves grown under intermediary light intensities. The latter value was chosen for use because the age and growth conditions of the leaves investigated resemble more closely those of Franck et al. (2002) than those used by Pfündel (1998).

With calculated spectra of PS I relative to  $F_M$  or  $F_0$  fluorescence (Eqs. 7 and 8), relative fluorescence excitation spectra of both photosystems can be derived from  $F_M(\lambda_{EX})$  as well as from  $F_0(\lambda_{EX})$  spectra. Here, the equations for  $F_0(\lambda_{EX})$  are presented:

$$F^{PS1}(\lambda_{EX}) = \frac{F_0(\lambda_{EX})}{I_{REL}(\lambda_{EX})} \cdot \left(\frac{F^{PS1}(\lambda_{EX})}{F_0(\lambda_{EX})}\right)_{\text{Equation 8}}, \tag{9}$$

$$F^{PS2}(\lambda_{EX}) = \frac{F_0(\lambda_{EX})}{I_{REL}(\lambda_{EX})} \cdot \left(1 - \left(\frac{F^{PS1}(\lambda_{EX})}{F_0(\lambda_{EX})}\right)_{\text{Equation 8}}\right). \tag{10}$$

Note that the calculation of excitation spectra of pure photosystems (Eqs. 9 and 10) requires that the leaf excitation spectrum,  $F_0(\lambda_{EX})$ , is corrected for the wavelength-dependent variations of the quantum flux densities of excitation light,  $I_{REL}(\lambda_{EX})$ .

Results

Fluorescence excitation spectra

The curves in Fig. 1a depict the spectra of fluorescence excitation light for the 33 filter settings used (400–720 nm at 10 nm increments). Frequently, the peak wavelengths of light spectra deviated from the decadic filter settings, and the positions of relative photon flux densities (dots in Fig. 1a) deviated from the respective peak positions of spectra (see Materials and methods for calculation of wavelengths). For simplicity, the decadic numbers of the filter settings will be used throughout the text except for the 690 nm setting which corresponds to an effective wavelength of 685 nm.

In Fig. 1a, spectra for the lowest and highest wavelength settings are not apparent because these spectra coincided with the zero line due to the low transmittance of long-pass and short-pass filters of the measuring light path (cf. Materials and methods). From 420 to 520 nm, the increase in peak height of spectra results from the increase in maximum transmittance of the GG19 glass filter and the tunable filter as specified by the manufacturer. Accordingly, the corresponding relative photon flux densities increase. The increase in relative photon flux densities from 560 to 670 nm, however, is determined by the increasing band width of measuring light. Decreasing relative photon

flux densities at wavelengths above 670 nm are caused by the short-pass filters in the measuring light path. The prominent peaks at 490 and 530 nm in the spectrum of relative photo flux density result from the two green emission bands of the xenon flash lamp (cf. Suggett et al. 2003).

In order to demonstrate the original excitation spectra obtained with the tunable filter, data from the wild-type barley leaf (cultivar “Donaria”) are used (Fig. 1b). Clearly, the  $F_M$  signal is much higher than the  $F_0$  signal except at border regions near 400 and 700 nm. Both  $F_M$  and  $F_0$  spectra are strongly affected by the spectrum of photon flux density: for instance, the xenon lamp emission peaks at 490 and 530 nm are well reproduced in the excitation spectra (compare Fig. 1a, b).

In the absence of a leaf sample, a weak and virtually wavelength-independent signal was observed which corresponds to the baseline signal of the fluorimeter (Schreiber et al. 1993). At lowest and highest wavelengths, at which excitation light intensity was zero, baseline and leaf signals coincided (Fig. 1b). Therefore, the level of the baseline signal can be considered as representative for the baseline signal contributing to leaf fluorescence and, consequently, it was subtracted from all fluorescence data prior to any data manipulation. Subsequently, the effects of various photon flux densities were removed by dividing each original excitation spectra by the spectrum of the relevant photon flux density.

For all three leaf types, Fig. 2 shows the corrected excitation spectra for  $F_0$  and  $F_M$  fluorescence after normalization to the long-wavelength maximum. The  $F_0$  and  $F_M$  spectra from the wild-type barley and maize leaf share similar spectral properties: excitation peaks were observed at 440, 480, 610, and 660 nm. The spectrum recorded with the Chl *b*-less barley leaf showed high values around 440 nm, lacked the 480 nm peak, exhibited a new peak at 500 nm, and the red peak was shifted 10 to 670 nm.

Clear differences between normalized  $F_0$  and  $F_M$  spectra from the wild-type barley leaf were only apparent in 510–530 nm range where the  $F_0$  was higher than the  $F_M$  (Fig. 2a). In the maize leaf, the  $F_0$  was higher than the  $F_M$  from 510 to 640 nm and in the Chl *b*-less barley leaf from 430 to 650 nm (Fig. 2b, c).

### Spectra of $F_V/F_M$

According to Eq. 6, the ratio of  $F_V/F_M$  is positively related to the PS II-to-PS I absorption ratio. Thus, a maximum in a spectrum of  $F_V/F_M$  points to high PS II absorption relative to PS I. The  $F_V/F_M$  is a rather robust and reliable fluorescence ratio because its calculation cancels out the

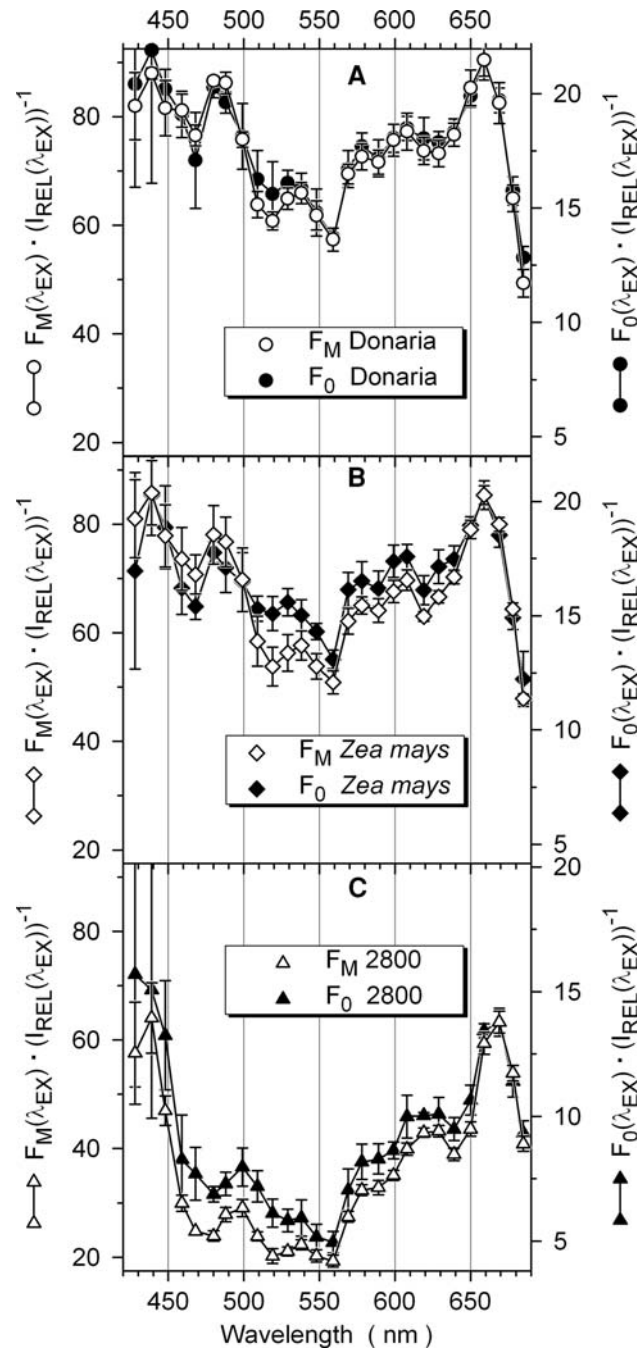


**Fig. 2** Relative quantum-corrected excitation spectra for  $F_0$  and  $F_M$  fluorescence. Spectra recorded with a wild-type barley (“Donaria”), a maize (“*Zea mays*”), and a Chl *b*-less barley leaf (“2800”) are shown in panels (a), (b), and (c), respectively. Solid symbols illustrate  $F_0$  data and open symbols display  $F_M$  data. All three panels possess identically scaled  $F_M$  axes (left ordinate axes). For each panel,  $F_0$  axis (right y axes) are scaled in such a way that the long-wavelength  $F_0$  maximum coincides with the long-wavelength  $F_M$  maximum. (Always, the zero points of parallel  $F_0$  and  $F_M$  axes coincide.) Data below 420 nm and above 690 nm were imprecise due to low excitation light intensities (cf. Fig. 1) and, thus, are not displayed. Error bars indicate 95% confidence (see Fig. 1)

influences of varying photon flux densities of measuring light and the effects of leaf optical properties so that the absolute values for  $F_V/F_M$  from different samples can be directly compared. Therefore, not the differences between spectra of  $F_0$  and  $F_M$  (Fig. 2) but the  $F_V/F_M$  data are used for statistical evaluations. All other spectral data, particularly the fluorescence excitation spectra of PS I and PS II (Figs. 5, 6), should be viewed against the background of  $F_V/F_M$  statistics.

Two principal statistical comparisons were carried out: first, “intra-spectral” statistics tests if the  $F_V/F_M$  varies significantly with wavelength within a spectrum and; second, “inter-spectral” statistics examines if the  $F_V/F_M$  at the same wavelength varies significantly between spectra. In the case of intra-spectral analysis (see Fig. 3), only extreme values having statistically different neighbors will be reviewed. In Fig. 3, such extreme values are connected to their statistically differing neighbors by thick gray lines. For inter-spectral statistics, the  $F_V/F_M$  spectrum from the barley wild-type leaf was chosen as the reference and differences between spectra are indicated by filled symbols on top of panels a and b.

The  $F_V/F_M$  spectrum of the barley wild-type leaf showed a maximum at 490 nm and the closest significantly different neighbors were located at 450 and 520 nm (Fig. 3a). Another maximum was positioned at 650 nm with significantly different data points at 630 and 680 nm. The significantly higher neighbors of the 520 nm minimum were located at 490 and 650 nm.

The  $F_V/F_M$  spectrum of the maize leaf exhibited a maximum at 470 nm instead of the 490 nm maximum observed with wild-type barley. The shape of the maize and the barley wild-type spectrum, however, was similar in the 450–500 nm range (Fig. 3a). The  $F_V/F_M$  of the maize leaf increased from 630 to the long wavelength maximum at 680 nm which had significantly different neighbors at 650 and 685 nm. The 650 nm value, in turn, was significantly higher than the minimum at 630 nm. As in wild-type barley, a 520 nm minimum existed in the maize  $F_V/F_M$  spectrum but the 520 nm minimum in maize was more pronounced and statistically different neighbors were found in closer proximity at 510 and 540 nm.

The  $F_V/F_M$  spectrum of the Chl *b*-less barley leaf exhibited a maximum at 490 nm with significantly different neighbors at 480 and 520 nm. Generally, in the 450–550 nm range, the spectrum of the Chl *b*-less mutant exhibited lower values of  $F_V/F_M$  and different shape compared to the wild-type barley (Fig. 3b). Similar to the maize leaf, a maximum at 680 nm was observed which had significantly differing neighbors at 660 and 685 nm (Fig. 3b). A new peak at 630 nm in the  $F_V/F_M$  spectrum of

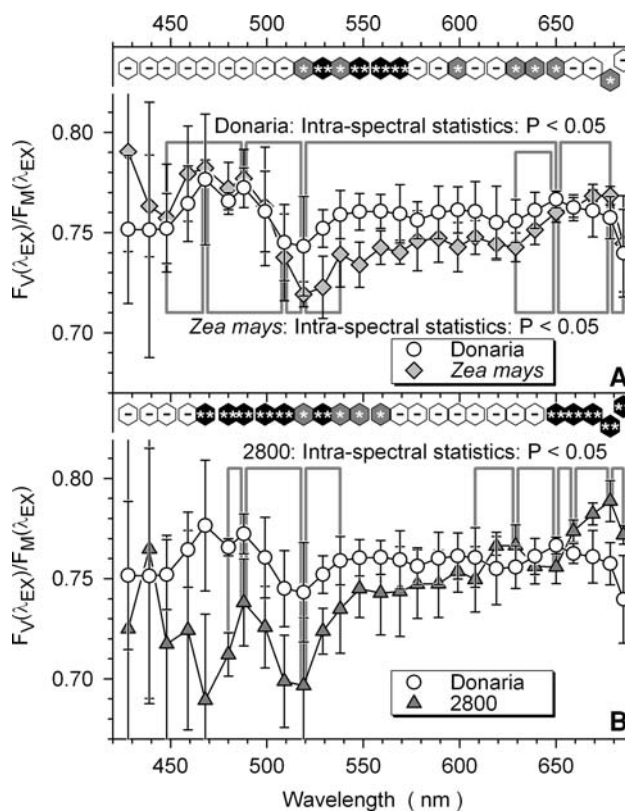


**Fig. 3** Spectra of  $F_V/F_M$ . The  $F_V/F_M$  spectrum of the barley wild-type leaf (open circles, “Donaria”) is drawn in both panels. The second spectrum in panel A is the  $F_V/F_M$  of the maize leaf (filled squares, “Zea mays”), and, in panel (b), the  $F_V/F_M$  of the Chl *b*-less barley leaf (filled triangles, “2800”). For each pair of spectra, differences were statistically analyzed by comparing the  $F_V/F_M$  data for each excitation wavelength (“inter-spectral” statistics). The results of inter-spectral analyses are displayed on top of each panel: the “-” sign indicates a  $P$  value  $> 0.05$ . The “\*”, and the “\*\*\*” signs signify  $0.01 \leq P < 0.05$ , and  $P < 0.01$ , respectively. Further, differences within each of the three spectra of  $F_V/F_M$  were evaluated (intra-spectral statistics): The results of intra-spectral statistics are illustrated by connecting with thick gray lines the nearest neighboring pairs of data points differing at a significance level of  $P < 0.05$ . The results of intra-spectral analyses of data from wild-type barley and maize leaves are represented above and below, respectively, the two spectra in panel (a). The outcome of intra-spectral analysis of data from the Chl *b*-less barley leaf is shown in (b). Bars indicate 95% confidence intervals (see Fig. 1)

the Chl *b*-less mutant was observed with significantly lower neighbors at 610 and 650 nm. The 650 nm value itself represented a minimum with significantly higher neighbors at 630 and 660 nm.

Compared to the wild-type barley leaf, the maize  $F_V/F_M$  was significantly lower from 520 to 570, at 600, and from 630 to 650 nm but it was significantly higher at 680 nm (Fig. 3a). In relation to the wild type, the Chl *b*-less mutant leaf exhibited significantly lower values of  $F_V/F_M$  from 470 to 560 and at 650 but was significantly higher from 660 to 685 nm (Fig. 3b).

## Spectra of PS I contribution to total leaf fluorescence

The relative PS I contribution to the total  $F_M$  and  $F_0$  fluorescence was calculated according to Eqs. 7 and 8, respectively, from  $F_V/F_M$  spectra (Fig. 3) using a value of 0.83 for  $\Phi_V^{PS2}$  (the  $F_V/F_M$  of pure PS II according to Franck et al. 2002). Generally, spectra of PS I to total fluorescence resembled the inverted corresponding spectra for  $F_V/F_M$  (compare Figs. 3, 4). The percentage of PS I fluorescence ranged between 5% and 17% at the  $F_M$  level (Fig. 4a, b) and between 21% and 54% at the  $F_0$  level (Fig. 4c, d). Overall, the conclusions of statistics on  $F_V/F_M$  data apply also for the spectra of PS I to total fluorescence but the relationships within and between spectra are inverted.

## In vivo fluorescence excitation spectra of PS I and PS II

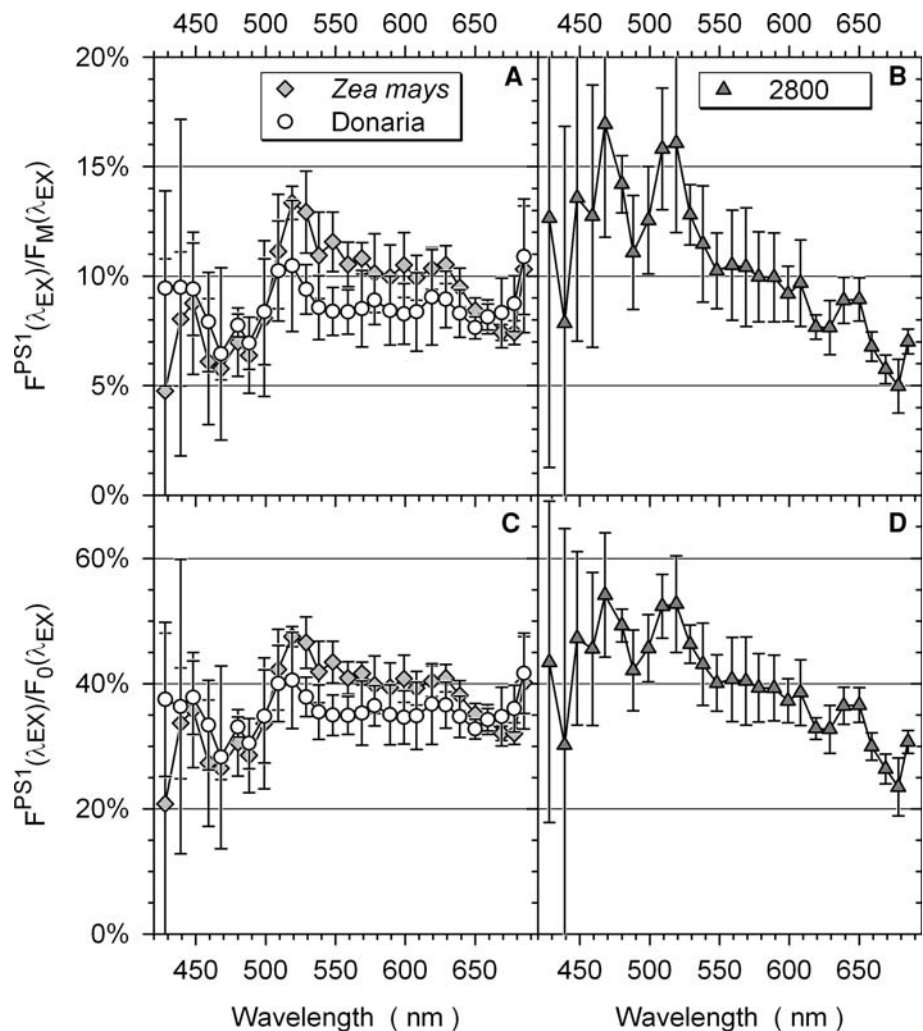
PS I excitation spectra were calculated according to Eq. 9 that is quantum-corrected excitation spectra for  $F_0$  fluorescence (Fig. 2) were multiplied by the corresponding

spectra of PS I contribution to total  $F_0$  fluorescence (Fig. 4). The PS II excitation spectrum is calculated in an analogous manner from Eq. 10. Note that the sum of PS I and PS II excitation spectra yields the original quantum-corrected excitation spectrum for  $F_0$  fluorescence.

For every leaf investigated, non-normalized PS II spectra are depicted in Fig. 5a–c. The parallel PS I spectra are normalized so that their long-wavelength peak intensity coincide with that of the PS II spectrum. Normalization of spectra aids visual comparison of PS I with PS II spectra but is principally arbitrary. Therefore, even clear differences between normalized PS I and PS II spectra do not necessarily indicate that the in vivo spectra also differ. Since Eq. 6 predicts that the spectra of  $F_V/F_M$  indicate spectral variations in the PS I to PS II absorption ratios, the comparison of the normalized PS I and PS II spectra will focus on those wavelengths at which statistically significant variations in spectra of  $F_V/F_M$  exist (Fig. 3).

Between 470–490 nm and at 650 nm, the PS II spectrum from the barley wild-type leaf exhibited higher values than

**Fig. 4** Spectra of percental contribution of PS I fluorescence to total fluorescence at  $F_M$  (a and b) and  $F_0$  levels (c and d). Left-handed panels depict data from the wild-type barley leaf (“Donaria,” open circles) and the maize leaf (“*Zea mays*,” filled squares). Panels on the right side represent data from the Chl *b*-less barley leaf (“2800,” filled triangles). Contributions of PS I fluorescence to total  $F_M$  and  $F_0$  level fluorescence were derived from data of  $F_V/F_M$  data (Fig. 3) using Eqs. 7 and 8, respectively, and the value of 0.83 for the in vivo  $F_V/F_M$  ( $\Phi_V^{PS2}$ ) of pure PS II as published by Franck et al. (2002). Bars indicate 95% confidence intervals (see Fig. 1)





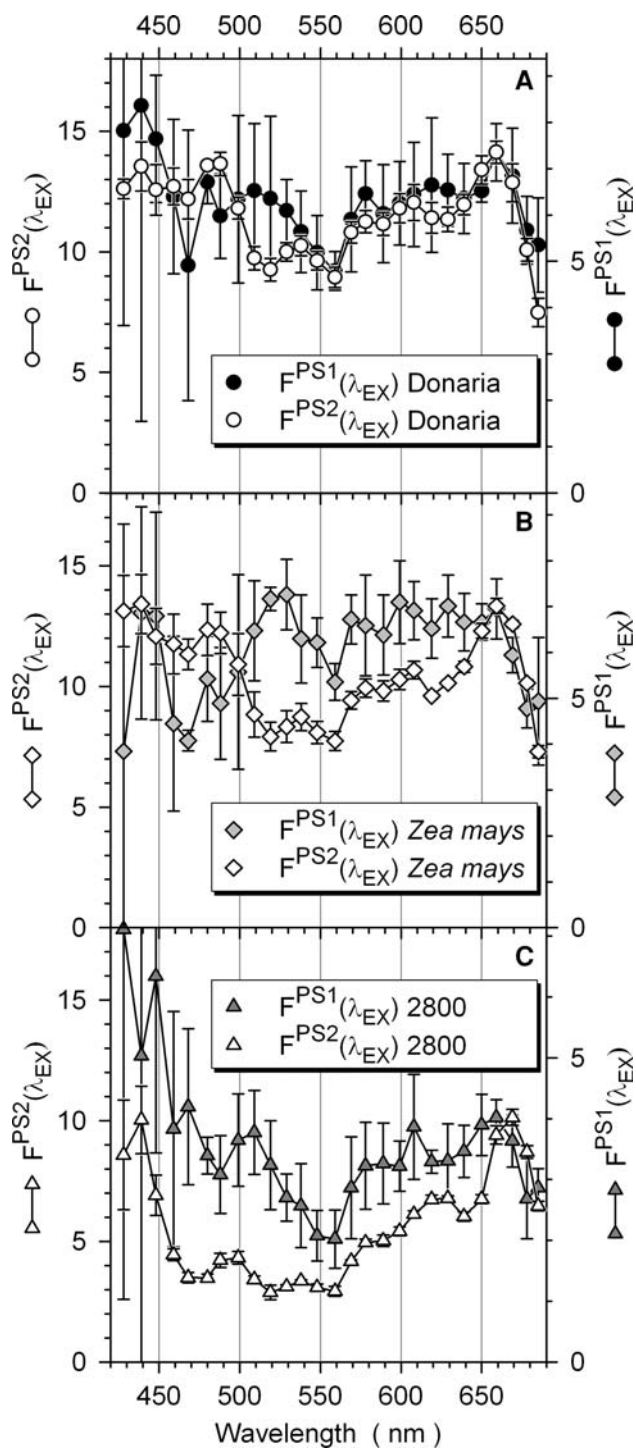


**Fig. 5** In vivo excitation spectra of PS I and PS II. The spectra of  $F^{PS1}(\lambda_{EX})$  (filled symbols) and  $F^{PS2}(\lambda_{EX})$  (open symbols) are derived from excitation spectra for  $F_0$  fluorescence (Fig. 2) and the spectra for relative PS I contribution to total fluorescence (Fig. 4) according to Eqs. 9 and 10, respectively. **a** Wild-type barley leaf, “Donaria”; **b** Maize leaf, “*Zea mays*”; **c** Chl *b*-less barley leaf, “2800.” All panels use the same ordinates for  $F^{PS2}(\lambda_{EX})$  (left-handed Y axes). The  $F^{PS1}(\lambda_{EX})$  ordinates (right-handed Y axis) are adjusted so that the height of long-wavelength peak of  $F^{PS1}(\lambda_{EX})$  and  $F^{PS2}(\lambda_{EX})$  coincide. Bars indicate 95% confidence intervals (see Fig. 1)

the corresponding PS I spectrum which correlates with the statistically meaningful  $F_V/F_M$  maxima at 490 and 650 nm, respectively (compare Figs. 3a, 5a). On the other hand, lower PS II than PS I fluorescence at excitation wavelengths 510–530 nm explains the 520 nm minimum in the barley wild-type  $F_V/F_M$  spectrum.

Between 460–490 nm and 670–680 nm, in the maize leaf the PS II spectrum was higher than the PS I spectrum which coincides with the maxima at 470 nm and 680 nm of the  $F_V/F_M$  spectrum (see Figs. 3a, 5b). Further, a maximum between 520 and 530 nm in the PS I spectrum, which occurred in parallel with low PS II fluorescence values, corresponds to the 520 nm minimum of the maize  $F_V/F_M$ . Notably, from 680 to 685 nm, the maize PS II fluorescence decreased but the PS I fluorescence increased slightly which explains the drop in  $F_V/F_M$  from 680 to 685 nm. In wild-type barley, the relationship between the spectra from the two photosystems at 680–685 nm was roughly comparable to maize but a significant variation in the  $F_V/F_M$  was not observed (Figs. 3a, 5a).

Except at 670 and 680 nm, the PS II spectrum from the barley Chl *b*-less mutant leaf exhibited lower values than the corresponding PS I spectrum. Apparently, the  $F_V/F_M$  maxima at 490 and 630 nm (Fig. 3b) correspond to troughs in the PS I spectrum which were paralleled by peaks in the PS II spectrum (Figs. 3b, 5c). Furthermore, the PS I maximum at 510 nm together with the PS II minimum at 520 nm explains the minimum in  $F_V/F_M$  at 520 nm. At longer wavelengths,  $F_V/F_M$  maximum from the mutant at 680 nm can be attributed to the PS II band at 670, which was red-shifted relative to the PS I maximum, and an increase in the PS I signal from 680 to 685 nm.

For direct comparison of excitation spectra of PS II or of PS I from the three different types of leaves, non-normalized PS II and PS I spectra are grouped in Fig. 6a and b, respectively. Wild-type barley and the maize leaves exhibited similar PS II spectra and approximately comparable PS I spectra. Mostly, the PS II fluorescence values were higher in the wild-type barley than in the maize leaf, whereas, in the 520–650 nm range, the PS I data were lower in wild-type barley than in the maize leaf. The latter differences explain why, in the 520–650 nm range, many  $F_V/F_M$  values were higher in wild-type barley than in maize (Fig. 3a). Between 670 and 685 nm, the PS I data from wild-type barley were higher than that from maize whereas the PS II data were similar. This is consistent with the higher  $F_V/F_M$  at 680 nm in maize than in wild-type barley.

Compared to wild-type barley, the Chl *b*-less mutant leaf exhibited lower PS II values in the 470–560 nm range (average reduction: 68%) while the PS I data were decreased to a lesser degree (average reduction: 47%;

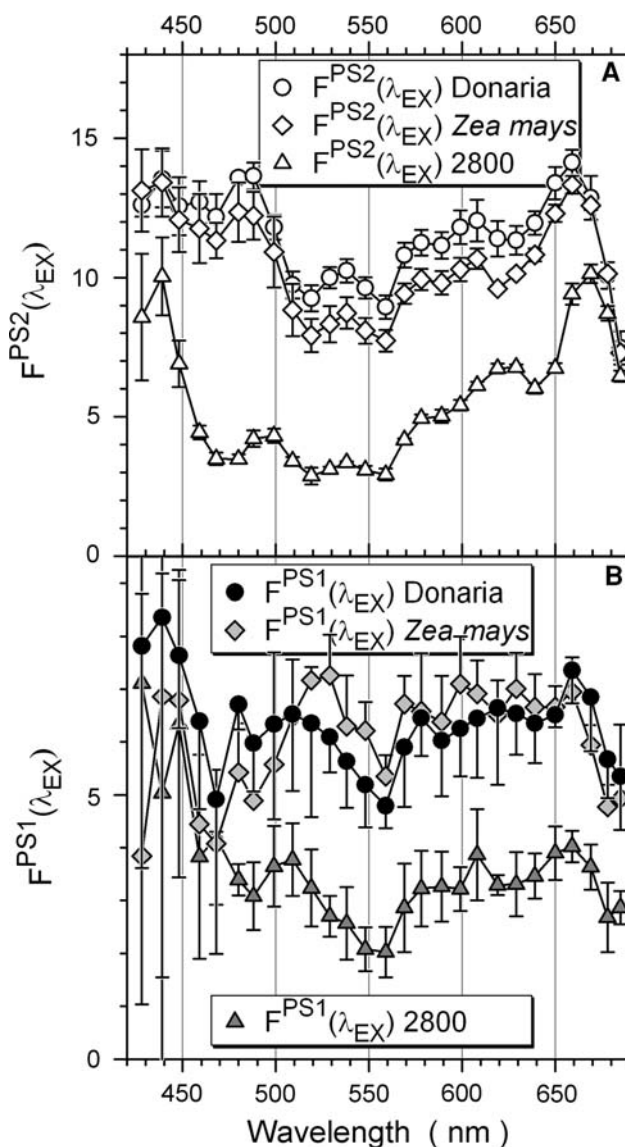


**Fig. 6** In vivo excitation spectra of PS I and PS II. Spectra of Fig. 5 are grouped in PS II (a) and PS I (b) curves. All spectra are non-normalized

Fig. 6a, b). The stronger reduction in PS II fluorescence explains why the  $F_V/F_M$  values from 470 to 560 nm are lower in the barley Chl *b* mutant than in the wild-type leaf (Fig. 3b). From 650 to 660 nm, PS II data in the barley mutant, but not in the wild type, increased steeply. This increase matches the changed  $F_V/F_M$  value of the barley Chl *b*-less mutant from significantly lower to significantly higher than that of the wild type (Fig. 3b). Between 660 and 685 nm, the Chl *b*-less mutant PS II signal was reduced on average by 26% but PS I values were reduced on average by 46% (Fig. 6) which explains the higher  $F_V/F_M$  in the mutant compared to the wild-type barley in this spectral range.

## Discussion

This study provides evidence that the  $F_V/F_M$  measured at ambient temperature depends on the wavelength of the exciting light (Fig. 3). According to the model introduced here, the wavelength dependency of  $F_V/F_M$  originates in the different excitation spectra for PS I and PS II fluorescence. Thus, if theory is correct, the PS I and PS II spectra derived from spectra of  $F_V/F_M$  (Figs. 5, 6) should resemble published spectra of photosystems.

Detailed action spectra of PS I and PS II have been recorded with dilute suspensions of higher plants chloroplasts (Boichenko 1998) or unicellular green algae (Ried 1971; Schreiber and Vidaver 1974) which are evolutionarily related to higher plants (Green and Durnford 1996). The fact that action and the fluorescence excitation spectra recorded here are absorbance-type spectra (absorbance = 1 – transmittance – reflectance) suggests that they should be comparable with each other.

Green leaves, however, contain higher concentrations of photosynthetic pigments than dilute chloroplast or cell suspensions. As a consequence, leaf spectra are expected to deviate from spectra of diluted suspensions for at least two reasons: firstly, according to the Beer–Lambert law, the transmittance of a sample is logarithmically related to its absorbance which itself varies proportionally with pigment concentration. Hence, the range of low absorption around 550 nm of dilute chloroplast suspensions (e.g., Boichenko 1998) is more elevated in leaf spectra compared to peak regions which exhibit high absorbance values already in dilute suspensions.

Secondly, at wavelengths of low pigment absorption, non-absorbed light is more frequently scattered inside the leaf than at wavelengths of high pigment absorption. This so-called “detour effect” elongates the effective optical path and thereby increases the probability of being absorbed by pigments particularly at wavelengths of low pigment absorption (Butler 1962; Rühle and Wild 1979). In fact, it has been estimated that the detour effect enlarges the leaf’s effective path length in the green (at minimum pigment absorption) by a factor of five compared to that of maximum pigment absorption in the blue and red (Vogelmann 1993). Hence, also the detour effect is responsible for elevation of leaf absorption of light at regions of low pigment absorption. In fact, Rivadossi et al. (1999) have derived from spectral simulations that the detour effect represents a major optical component of leaf absorption spectra.

A conspicuous example illustrating the differences between leaf and dilute suspensions is the long-wavelength maximum: in excitation spectra of the wild-type barley and the maize leaf, the peak occurs at 660 nm (Fig. 2a, b) while the peak in absorption spectra from suspensions of

chloroplasts from higher plants and green algae occurs at 680 nm (Cho and Govindjee 1970; Rivadossi et al. 1999). Similar to the present data, the adaxially excited and detected fluorescence excitation spectrum from bean leaves peaked at 650 nm but the shape of this band was relatively broad and asymmetrical (Louis et al. 2006). Using very dense chloroplasts preparations, also Govindjee and Yang (1966) have observed that fluorescence excitation spectra recorded at room temperature showed an asymmetrical band with a blue-shifted maximum near 650 nm. The authors have tentatively attributed this blue-shift to the detour effect. Taking up the idea by Govindjee and Yang (1966), also the blue-shift of the long-wavelength maximum in the present excitation spectra might originate in the detour effect.

It is noteworthy that the short-wavelength excitation maximum of wild-type barley and the maize excitation spectra was located at 440 nm (Fig. 2a, b) and, thus, agrees with literature (Cho and Govindjee 1970; Rivadossi et al. 1999). This can be explained by considering that marked distortion of pigment spectra by the detour effect requires steep spectral changes in the effective optical path length caused by steep spectral absorption changes of pigments. The latter condition is present at the long wavelength maximum at which pigment absorption drops steeply toward shorter wavelengths but not at the short-wavelength maximum which is situated right within the broad blue absorption band (cf. Cho and Govindjee 1970; Inada 1980; Rivadossi et al. 1999).

The long-wavelength excitation maximum of the Chl *b*-free barley leaf occurred at 670 nm but the corresponding wild type peak at 660 nm (Fig. 2c). Because the *in vivo* position of the long-wavelength maximum of Chl *b* is located around 650 nm (Cho and Govindjee 1970; French et al. 1972), it is tempting to speculate that the lack of Chl *b* absorption shifts the 660 nm maximum of the wild type to 670 nm. Barley Chl *b*-less mutant leaves, however, contain much lower total chlorophyll concentrations than wild type leaves (Andrews et al. 1995; Falk et al. 1994). Different pigment concentrations in wild type and mutant leaves will certainly result in different pigment absorption properties which, in turn, bring about different spectral behavior of the detour effect. Therefore, variations in the detour effect might similarly explain the different position of the long-wavelength maximum in mutant and wild-type excitation spectra.

It must also be considered that all photosystem spectra were derived from spectra of  $F_V/F_M$  using the same  $\Phi_V^{\text{PS2}}$  ( $\Phi_V^{\text{PS2}} = F_V/F_M$  of pure PS II). This practice is based on the observation that fluorescence data from mature leaves of various biochemical types of photosynthesis matched the same linear function which was derived by assuming a constant  $\Phi_V^{\text{PS2}}$  (Pfundel 1998). Also, that  $\Phi_V^{\text{PS2}}$  established

by Franck et al. (2002) was used to derive spectra of photosystems and not the higher  $\Phi_V^{\text{PS2}}$  estimated earlier by Pfundel (1998) is supported by the range of PS I contributions to total fluorescence (Fig. 4) which agrees well with published data (see references in Introduction).

#### PS I and PS II spectra

Despite the influence of leaf optical properties discussed above, between 450 and 500 nm, the PS I and PS II spectra from wild-type barley and maize resembled the published spectra: both leaf PS II spectra showed a broad peak from 480 to 490 nm which was roughly as high as the 440 nm maximum (Fig. 6a). In comparison, the absorption spectrum of isolated PS II preparations showed a broad band at similar wavelengths which has been attributed to light absorption by Chl *b* and carotenoids of the LHC II, the major light-harvesting antenna of PS II (Siefermann-Harms 1985; Rivadossi et al. 1999). The corresponding PS I band peaked at 480 nm, lacked prominent 490 nm absorption and tended to be smaller than the PS I 440 nm maximum (Fig. 6b). The relative small bandwidth of the 480 nm PS I peak is consistent with the absorption spectral details of isolated PS I complexes (Croce et al. 1996; 2002; Kargul et al. 2003) and of PS I action spectra derived from isolated chloroplasts (Boichenko 1998). The higher PS II 480–490 nm peak compared to the PS I 480 nm peak (Fig. 5a, b) is also consistent with the differences between PS I and PS II action spectra in chloroplasts (Boichenko 1998; Loos 1976) and green algal suspensions (Ried 1971; Schreiber and Vidaver 1974). Both, the small intensity and narrow shape of the 480 nm peak of the PS I spectrum is in agreement with the low Chl *b* and xanthophyll concentrations in the PS I holo-complex (Siefermann-Harms 1985).

In the Chl *b*-less mutant leaf, the PS II 480–490 nm band is missing which is consistent with its small PS II antenna size (Ghirardi et al. 1986; Falk et al. 1994) caused by the failure to accumulate significant amounts of LHC-II proteins (Preiss and Thornber 1995). That the mutant PS I spectrum lacks the 480 nm peak of the wild-type wild can be explained by the absence of Chl *b* absorption: the remaining absorption in the 480–490 nm range can be ascribed to carotenoids (cf. Cho and Govindjee 1970; Siefermann-Harms 1985). In the mutant, the moderate reduction of the 450–500 nm absorption of PS I is consistent with some accumulation of proteins of LHC I in the absence of Chl *b* (Preiss and Thornber 1995), but also because a large part of the PS I antenna is associated with the PS I core complex (Melis 1991; Scheller et al. 2001).

Between 500 and 550 nm, the PS I spectra differed from PS II by exhibiting a clear band at 530 nm in the maize leaf and at 510 nm in the other two leaves (Figs. 5, 6b). A comparable peak at 515 nm has been observed in the PS I

minus PS II difference of fluorescence excitation spectra from spinach chloroplasts recorded at 77 K by Kitajima and Butler (1975b) which was tentatively attributed to a carotenoid of PS I. Also, action spectra from the green macroalga *Ulva lobata* showed PS I-specific bands in the 500–530 nm range (Vidaver 1966; Vidaver and French 1965). A similarly pronounced carotenoid band between 500 and 550 nm, however, is not apparent in absorption and fluorescence excitation spectra of the isolated PS I (Croce et al. 1996; Rivadossi et al. 1999) and action spectra measured with chloroplast or algal cell suspensions (Ried 1971; Schreiber and Vidaver 1974; Boichenko 1998). Contrary to the data presented here, Evans (1987) has reported a shoulder at 525 nm in PS II to PS I absorption ratios derived from the wavelength dependence of photosynthetic quantum yield in higher plants. A provisional explanation for the variable appearance of a band between 500 and 550 nm is that the small shoulders present in the fluorescence excitation spectrum of the isolated PS I (Croce et al. 1996) are variably amplified depending on sample optics and the optical peculiarities of the experimental arrangement (cf. Louis et al. 2006).

The PS II spectrum from the barley Chl *b*-less mutant leaf exhibited a band at 500 nm (Fig. 5c) which possibly arises, as earlier suggested (Pfündel and Baake 1990; Pfündel et al. 2007), from carotenes which transfer excitation energy to PS II in combination with light-screening xanthophylls absorbing at shorter wavelengths than 500 nm.

Between 550 and 650 nm, the PS I spectrum from the wild-type barley leaf was higher than the PS II spectrum and revealed a maximum at 620 nm (Fig. 5a) which is consistent with the markedly higher Chl *a*/Chl *b* ratios in PS I than in PS II (Siefermann-Harms 1985) and the approximately 1.5 fold higher molar absorptivity of the 620 nm Chl *a* absorption band compared to the relevant Chl *b* band (Cerovic et al. 1999). Generally, the tendency of higher PS I than PS II spectral data between 550 and 650 nm agrees with the low PS II to PS I absorption ratios at these wavelengths as observed with leaves from other plant species (Evans 1987). In green algal suspensions, however, variable relationships between PS I and PS II spectra between 550 and 650 nm have been observed: after normalization to the red maximum, the PS I action spectrum was higher (Schreiber and Vidaver 1974) or lower (Ried 1971) than the PS II action spectrum. The difference between the two studies might be related to different physiological states of the algae studied (cf. Ried 1971). Also, with chloroplast suspensions, the relationship between PS I and PS II action spectra is variable depending on thylakoid stacking and LHC II phosphorylation (Boichenko 1998). Therefore, the higher PS I than PS II absorption between 550 and 650 nm might be a property of the dark-acclimated barley leaf investigated here.

In the maize leaf, the 550–650 nm PS I spectrum was markedly higher than the PS II spectrum (Fig. 5b), but PS I and PS II spectra differed only slightly in the barley wild-type leaf (Fig. 5a). Moreover, the PS I values at 550–650 nm were higher in maize compared to wild-type barley (Fig. 6b). Both observations are consistent with the higher PS I/PS II concentration ratios in leaves of NADP-ME C<sub>4</sub>-type plants like maize than in barley leaves with C<sub>3</sub> photosynthesis (Edwards and Walker 1983, Pfündel and Neubohn 1999). Possibly, specific leaf optical properties associated to the Kranz anatomy of the maize leaf might further improve light absorption by PS I. Also both, different PS I concentrations and leaf optical properties, may explain why the  $F_0$  and  $F_M$  spectra differ more clearly in maize than in wild-type barley (Fig. 2a, b).

Also in the barley Chl *b*-less mutant leaf, at 550–650 nm, the PS I spectrum was markedly higher than PS II (Fig. 5c). Similar as in maize, the relatively high PS I absorption can be explained by concentration-dependent effects: the mutant has higher concentrations of PS I-associated than PS II associated pigments because the mutation diminished PS I antennae to a lesser degree than PS II antennae (Ghirardi et al. 1986; Falk et al. 1994).

The long-wavelength peaks of PS I and PS II spectra seem significantly affected by leaf optical properties (see above) and, thus, their comparison with other spectra is difficult. However, known spectral properties of the photosystems explain why the PS I spectra recorded with the maize and the Chl *b*-less mutant leaf slightly increased from 680 to 685 nm while the PS II spectra decreased steeply (Fig. 5b, c). Firstly, PS I action spectra peak around 685 nm and PS II action spectra around 680 nm (Boichenko 1998; Ried 1971; Schreiber and Vidaver 1974). Secondly, total pigment absorption in leaves drops steeply from 680 toward longer wavelengths (Inada 1980) resulting in an increase of the effective optical path length by the detour effect, which eventually emphasized PS I absorption. This effect is particularly apparent in maize and the Chl *b*-less barley; that is, in leaves with elevated PS I/PS II pigment concentration ratios.

To summarize, intra-spectral and inter-spectral variations of  $F_V/F_M$  (Fig. 3) can be generally explained by spectral properties of PS I and PS II. Specifically, light absorption by LHC II seems to give rise to the maxima between 470 and 490 nm in the  $F_V/F_M$  spectra of the wild-type barley and maize leaf, but light absorption by LHC II also explains the higher  $F_V/F_M$  data between 470 and 510 nm in wild type compared to the Chl *b*-less barley leaf. Further, a special PS I absorption band, supposedly due to PS I-associated carotenoids, causes minimum values of  $F_V/F_M$  around 520 nm in all three leaves investigated. Increased light absorption in the 550–650 nm region in the presence of increased PS I/PS II concentration ratios in

maize results in the lowered values of  $F_V/F_M$ . Finally, low values of  $F_V/F_M$  at 685 seem to originate in preferential PS I absorption at this wavelength. Therefore, the large agreement between  $F_V/F_M$ -derived photosystem spectra and published data supports the theoretical concept introduced here.

### Concluding remarks

This study strongly supports the idea that information on light absorption spectra of PS I and PS II can be non-destructively derived from the excitation wavelength dependence of  $F_V/F_M$ . Hence, measurements of spectra of  $F_V/F_M$  present themselves as a means to study how PS I and PS II absorption properties acclimates to various light environments but also to investigate the peculiarities of PS I and PS II light absorption in leaves possessing different anatomy and/or different biochemical types of photosynthesis. Considering that  $F_V/F_M$  is influenced by the extent of PS I light absorption, then an increase in PS I light absorption by LHC II binding during state transitions will result in a decreased  $F_V/F_M$  at wavelengths of prominent LHC II absorption. Therefore, a decrease in  $F_V/F_M$  during state 1–state 2 transition does not necessarily indicate decreased photochemical yield of PS II due to PS II-to-PS I energy spill-over as has been suggested earlier (Allen 1992).

This article reports a proof of principle study based on a limited number of measurements. The small number of data acquired was sufficient for statistical analysis but resulted in low accuracies of some mean values. Because determinations  $F_V/F_M$  are non-destructive, however, the accuracy of mean values can be easily improved by increasing the number of leaf scans. Also, the spectral resolution of  $F_V/F_M$  data can be significantly improved by employing a tunable filter with narrower band widths of transmission windows. Compared to the latter option, a less expensive way to study spectral variations in  $F_V/F_M$  is the use of a range of narrow-bands selected according to a particular research focus.

**Acknowledgements** I am grateful to Dr. Robert J. Porra, CSIRO-Plant Industry, Canberra, Australia, for help in preparing this manuscript. I thank LOT-Oriel, Germany, for supplying me with a tunable filter.

### References

Agati G, Cerovic ZG, Moya I (2000) The effect of decreasing temperature up to chilling values on the in vivo F685/F735 chlorophyll fluorescence ratio in *Phaseolus vulgaris* and *Pisum sativum*: the role of the Photosystem I contribution to the 735 nm fluorescence band. *Photochem Photobiol* 72:75–84. doi:10.1562/0031-8655(2000)072<0075:TEODTU>2.0.CO;2

- Allen JF (1992) Protein phosphorylation in regulation of photosynthesis. *Biochim Biophys Acta* 1098:275–335
- Anderson JM, Melis A (1983) Localization of different photosystems in separate regions of chloroplast membranes. *Proc Natl Acad Sci USA* 80:745–749. doi:10.1073/pnas.80.3.745
- Andrews JR, Fryer MJ, Baker NR (1995) Consequences of LHC II deficiency for photosynthetic regulation in *chlorina* mutants of barley. *Photosynth Res* 44:81–91. doi:10.1007/BF00018299
- Baker NR (2008) Chlorophyll fluorescence: a probe of photosynthesis in vivo. *Annu Rev Plant Biol* 59:89–113. doi:10.1146/annurev.arplant.59.032607.092759
- Boichenko VA (1998) Action spectra and functional antenna sizes of Photosystems I and II in relation to the thylakoid membrane organization and pigment composition. *Photosynth Res* 58:163–174. doi:10.1023/A:1006187425058
- Butler WL (1962) Absorption of light by turbid materials. *J Opt Soc Am* 52:292–299. doi:10.1364/JOSA.52.000292
- Butler WL (1978) Energy distribution in the photochemical apparatus of photosynthesis. *Annu Rev Plant Physiol* 29:345–378. doi:10.1146/annurev.pp.29.060178.002021
- Butler WL, Kitajima M (1975) Energy transfer between photosystem II and photosystem I. *Biochim Biophys Acta* 396:72–85. doi:10.1016/0005-2728(75)90190-5
- Cerovic ZG, Samson G, Morales F, Tremblay N, Moya I (1999) Ultraviolet-induced fluorescence for plant monitoring: present state and prospects. *Agronomie* 19:543–578. doi:10.1051/agro:19990701
- Cho F, Govindjee (1970) Low-temperature (4–77 degrees K) spectroscopy of *Chlorella*: temperature dependence of energy transfer efficiency. *Biochim Biophys Acta* 216:139–150. doi:10.1016/0005-2728(70)90166-0
- Croce R, Zucchelli G, Garlaschi FM, Bassi R, Jennings RC (1996) Excited state equilibration in the photosystem I-light-harvesting I complex: P700 is almost isoenergetic with its antenna. *Biochemistry* 35:8572–8579. doi:10.1021/bi960214m
- Croce R, Morosinotto T, Castelletti S, Breton J, Bassi R (2002) The Lhca antenna complexes of higher plants photosystem I. *Biochim Biophys Acta* 1556:29–40. doi:10.1016/S0005-2728(02)00304-3
- Dau H (1994) Molecular mechanisms and quantitative models of variable photosystem II fluorescence. *Photochem Photobiol* 60:1–23
- Edwards G, Walker D (1983) C3, C4: mechanisms, and cellular and environmental regulation, of photosynthesis. Blackwell, Oxford
- Evans RE (1987) The dependence of quantum yield on wavelength and growth irradiance. *Aust J Plant Physiol* 14:69–79
- Falk S, Bruce D, Huner NPA (1994) Photosynthetic performance and fluorescence in relation to antenna size and absorption cross-sections in rye and barley grown under normal and intermittent light conditions. *Photosynth Res* 42:145–155. doi:10.1007/BF02187125
- Franck F, Juneau P, Popovic R (2002) Resolution of the Photosystem I and Photosystem II contributions to chlorophyll fluorescence of intact leaves at room temperature. *Biochim Biophys Acta* 1556:239–246. doi:10.1016/S0005-2728(02)00366-3
- French CS, Brown JS, Lawrence MC (1972) Four universal forms of chlorophyll a. *Plant Physiol* 49:421–429. doi:10.1104/pp.49.3.421
- Genty B, Wonders J, Baker NR (1990) Non-photochemical quenching of  $F_0$  in leaves is emission wavelength dependent: consequences for quenching analysis and its interpretation. *Photosynth Res* 26:133–139. doi:10.1007/BF00047085
- Ghirardi ML, McCauley SW, Melis A (1986) Photochemical apparatus organization in the thylakoid membrane of *Hordeum vulgare* wild type and chlorophyll *b*-less *chlorina* f2 mutant. *Biochim Biophys Acta* 851:331–339. doi:10.1016/0005-2728(86)90069-1

- Govindjee (2004) Chlorophyll *a* fluorescence: a bit of basics and history. In: Papageorgiou GC, Govindjee (eds) Chlorophyll *a* fluorescence: a signature of photosynthesis. Advances in photosynthesis and respiration, vol 19. Springer, Dordrecht, pp 1–41
- Govindjee, Yang L (1966) Structure of the red fluorescence band in chloroplasts. *J Gen Physiol* 49:763–780. doi:10.1085/jgp.49.4.763
- Green BR, Durnford DG (1996) The chlorophyll-carotenoid proteins of oxygenic photosynthesis. *Annu Rev Plant Physiol Plant Mol Biol* 47:685–714. doi:10.1146/annurev.arplant.47.1.685
- Haldrup A, Jensen PE, Lunde C, Scheller HV (2001) Balance of power: a view of the mechanism of photosynthetic state transitions. *Trends Plant Sci* 6:301–305. doi:10.1016/S1360-1385(01)01953-7
- Horton P, Black MT (1981) Light-dependent quenching of chlorophyll fluorescence in pea chloroplasts induced by adenosine 5'-triphosphate. *Biochim Biophys Acta* 635:53–62. doi:10.1016/0005-2728(81)90006-2
- Inada K (1980) Spectral absorption property of pigments in living leaves and its contribution to photosynthesis. *Jpn J Crop Sci* 49:286–294
- Joliot P, Joliot A, Kok B (1968) Analysis of the interactions between the two photosystems in isolated chloroplasts. *Biochim Biophys Acta* 153:635–652. doi:10.1016/0005-2728(68)90191-6
- Karageorgou P, Tziortzis I, Manetas Y (2007) Are saturating pulses indeed saturating? Evidence for considerable PSII yield underestimation in leaves adapted to high levels of natural light. *J Plant Physiol* 164:1331–1336. doi:10.1016/j.jplph.2006.07.015
- Kargul J, Nield J, Barber J (2003) Three-dimensional reconstruction of a light-harvesting complex I-photosystem I (LHCI-PSI) Supercomplex from the Green Alga *Chlamydomonas reinhardtii*. *J Biol Chem* 278:16135–16141. doi:10.1074/jbc.M300262200
- Kitajima M, Butler WL (1975a) Quenching of chlorophyll fluorescence and primary photochemistry in chloroplasts by dibromothymoquinone. *Biochim Biophys Acta* 376:105–115. doi:10.1016/0005-2728(75)90209-1
- Kitajima M, Butler WL (1975b) Excitation spectra for photosystem I and photosystem II in chloroplasts and the spectral characteristics of the distributions of quanta between the two photosystems. *Biochim Biophys Acta* 408:297–305. doi:10.1016/0005-2728(75)90131-0
- Krause GH, Jahns P (2004) Non-photochemical energy dissipation determined chlorophyll fluorescence quenching: characterization and function. In: Papageorgiou GC, Govindjee (eds) Chlorophyll *a* fluorescence: a signature of photosynthesis. Advances in photosynthesis and respiration, vol 19. Springer, Dordrecht, pp 463–495
- Loos E (1976) The effect of magnesium ions on action spectra for reactions mediated by photosystems I and II in spinach chloroplasts. *Biochim Biophys Acta* 440:314–321. doi:10.1016/0005-2728(76)90065-7
- Louis J, Cerovic ZG, Moya I (2006) Quantitative study of fluorescence excitation and emission spectra of bean leaves. *J Photochem Photobiol B Biol* 85:65–71. doi:10.1016/j.jphotobiol.2006.03.009
- Melis A (1991) Dynamics of photosynthetic membrane composition and function. *Biochim Biophys Acta* 1058:87–106. doi:10.1016/S0005-2728(05)80225-7
- Mukerji I, Sauer K (1989) Temperature-dependent steady-state and picosecond kinetic fluorescence measurements of a Photosystem I preparation from spinach. In: Briggs WR (ed) Photosynthesis. Alan R. Liss, Inc, New York, pp 105–122
- Peterson RB, Oja V, Laisk A (2001) Chlorophyll fluorescence at 680 and 730 nm and leaf photosynthesis. *Photosynth Res* 70:185–196. doi:10.1023/A:1017952500015
- Pfündel EE (1998) Estimating the contribution of Photosystem I to total leaf chlorophyll fluorescence. *Photosynth Res* 56:185–195. doi:10.1023/A:1006032804606
- Pfündel EE, Baake E (1990) A quantitative description of fluorescence excitation spectra in bean leaves greened under intermittent light. *Photosynth Res* 26:19–28
- Pfündel EE, Neubohn B (1999) Assessing photosystem I and II distribution in leaves from C<sub>4</sub> plants using confocal laser scanning microscopy. *Plant Cell Environ* 22:1569–1577. doi:10.1046/j.1365-3040.1999.00521.x
- Pfündel EE, Ben Ghazlen N, Meyer S, Zoran G, Cerovic ZG (2007) Investigating UV screening in leaves by two different types of portable UV fluorimeters reveals in vivo screening by anthocyanins and carotenoids. *Photosynth Res* 93:205–221. doi:10.1007/s11200-007-9135-7
- Preiss S, Thorber JP (1995) Stability of the apoproteins of light-harvesting complex I and II during biogenesis of thylakoids in the chlorophyll b-less barley mutant chlorine f2. *Plant Physiol* 107:709–717
- Rappaport F, Béal D, Joliot A, Joliot P (2007) On the advantages of using green light to study fluorescence yield changes in leaves. *Biochim Biophys Acta* 1767:56–65. doi:10.1016/j.bbabi.2006.10.002
- Ried A (1971) Improved action spectra of light reaction I and II. In: Forti G, Avron M, Melandri A (eds) IInd international congress on photosynthesis, Stresa, Italy. W. Junk, The Hague, pp 763–772
- Rivadossi A, Zucchelli G, Garlaschi FM, Jennings RC (1999) The importance of PSI chlorophyll red forms in light-harvesting by leaves. *Photosynth Res* 60:209–215. doi:10.1023/A:1006236829711
- Rühle W, Wild A (1979) The intensification of absorbance changes in leaves by light-dispersion. Differences between high-light and low-light leaves. *Planta* 146:551–557. doi:10.1007/BF00388831
- Scheller HV, Jensen PE, Haldrup A, Lunde C, Knoetzel J (2001) Role of subunits in eukaryotic Photosystem I. *Biochim Biophys Acta* 1507:41–60. doi:10.1016/S0005-2728(01)00196-7
- Schreiber U (2004) Pulse-amplitude-modulation (PAM) fluorometry and saturation pulse method: an overview. In: Papageorgiou GC, Govindjee (eds) Chlorophyll *a* fluorescence: a signature of photosynthesis. Advances in photosynthesis and respiration, vol 19. Springer, Dordrecht, pp 279–319
- Schreiber U, Vidaver W (1974) Chlorophyll fluorescence induction in anaerobic *Scenedesmus obliquus*. *Biochim Biophys Acta* 368:97–112. doi:10.1016/0005-2728(74)90100-5
- Schreiber U, Neubauer C, Schliwa U (1993) PAM fluorometer based on medium-frequency pulsed Xe-flash measuring light: a highly sensitive new tool in basic and applied photosynthesis research. *Photosynth Res* 36:65–72. doi:10.1007/BF00018076
- Sieffermann-Harms D (1985) Carotenoids in photosynthesis. I. Location in photosynthetic membranes and light-harvesting function. *Biochim Biophys Acta* 811:325–355
- Simpson DJ, Machold O, Hoyer-Hansen G, von Wettstein D (1985) Chlorina mutants of barley (*Hordeum vulgare* L.). *Carlsberg Res Commun* 50:223–238. doi:10.1007/BF02907148
- Suggett DJ, Oxborough K, Baker NR, MacIntyre HL, Kana TM, Geider RJ (2003) Fast repetition rate and pulse amplitude modulation chlorophyll *a* fluorescence measurements for assessment of photosynthesis electron transport in marine phytoplankton. *Eur J Phycol* 38:371–384. doi:10.1080/09670260310001612655
- Trissl HW (1997) Determination of the quenching efficiency of the oxidized primary donor of Photosystem I, P700<sup>+</sup>: implications for the trapping mechanism. *Photosynth Res* 54:237–240. doi:10.1023/A:1005981016835

- Trissl HW, Wilhelm C (1993) Why do thylakoid membrane stacks from higher plants form grana stacks. *Trends Biochem Sci* 18: 415–419. doi:[10.1016/0968-0004\(93\)90136-B](https://doi.org/10.1016/0968-0004(93)90136-B)
- Vidaver W (1966) Separate action spectra for the two photochemical systems of photosynthesis. *Plant Physiol* 41:87–89. doi:[10.1104/pp.41.1.87](https://doi.org/10.1104/pp.41.1.87)
- Vidaver W, French CS (1965) Oxygen uptake and evolution following monochromatic flashes in *Ulva* and an action spectrum for system I. *Plant Physiol* 40:7–12. doi:[10.1104/pp.40.1.7](https://doi.org/10.1104/pp.40.1.7)
- Vogelmann TC (1993) Plant tissue optics. *Annu Rev Plant Physiol Plant Mol Biol* 44:231–251. doi:[10.1146/annurev.pp.44.060193.001311](https://doi.org/10.1146/annurev.pp.44.060193.001311)
- Zucchelli G, Garlaschi FM, Jennings RC (1988) Influence of electrostatic screening by cations on energy coupling between Photosystem II reaction centres and the light-harvesting chlorophyll a/b protein complex II. *Biochim Biophys Acta* 934:144–150. doi:[10.1016/0005-2728\(88\)90129-6](https://doi.org/10.1016/0005-2728(88)90129-6)